



HAL
open science

Precision Measurements of Beta Spectra using Metallic Magnetic Calorimeters within the European Metrology Research Project MetroBeta

Martin Loidl, J. Beyer, L. Bockhorn, J. Bonaparte, C. Enss, S. Kempf, K. Kossert, Riham Mariam, O. Nähle, M. Paulsen, et al.

► **To cite this version:**

Martin Loidl, J. Beyer, L. Bockhorn, J. Bonaparte, C. Enss, et al.. Precision Measurements of Beta Spectra using Metallic Magnetic Calorimeters within the European Metrology Research Project MetroBeta. *Journal of Low Temperature Physics*, 2020, 199 (1-2), pp.451-460. 10.1007/s10909-020-02398-2 . cea-04567222

HAL Id: cea-04567222

<https://cea.hal.science/cea-04567222>

Submitted on 3 May 2024


HAL is a multi-disciplinary open access archive for the deposit and dissemination of scientific research documents, whether they are published or not. The documents may come from teaching and research institutions in France or abroad, or from public or private research centers.

L'archive ouverte pluridisciplinaire **HAL**, est destinée au dépôt et à la diffusion de documents scientifiques de niveau recherche, publiés ou non, émanant des établissements d'enseignement et de recherche français ou étrangers, des laboratoires publics ou privés.



Author Proof

1 **Precision Measurements of Beta Spectra using Metallic**
2 **Magnetic Calorimeters within the European Metrology**
3 **Research Project MetroBeta**

4 **M. Loidl¹  · J. Beyer² · L. Bockhorn^{3,5} · J. J. Bonaparte⁴ · C. Enss⁴ · S. Kempf⁴ ·**
5 **K. Kossert³ · R. Mariam¹ · O. Nähle³ · M. Paulsen^{2,4} · P. Ranitzsch³ ·**
6 **M. Rodrigues¹ · M. Wegner⁴**

7 Received: 19 July 2019 / Accepted: 8 February 2020
8 © Springer Science+Business Media, LLC, part of Springer Nature 2020

9 **Abstract**

10 MetroBeta, a recently completed European Metrology Research Project, aimed at
11 the improvement of the knowledge of the shapes of beta spectra, both in terms of
12 theoretical calculation and measurement. The most prominent experimental work
13 package concerned the measurement of the spectrum shapes of several beta decay-
14 ing radionuclides by means of metallic magnetic calorimeters (MMCs) with the beta
15 emitter embedded in the absorber. New MMC chips were designed and optimized
16 for five different absorber heat capacities, enabling the measurement of beta spectra
17 with Q values ranging from few tens of keV up to ~1 MeV. Several beta spectra
18 were measured with high energy resolution and statistics of up to 10^7 counts. A01
A02

19 **Keywords** Beta spectrometry · Metallic magnetic calorimeter · Radionuclide
20 metrology

A1 ✉ M. Loidl
A2 martin.loidl@cea.fr

A3 ¹ CEA, LIST, Laboratoire National Henri Becquerel (LNE-LNHB), CEA-Saclay,
A4 91191 Gif Sur Yvette Cedex, France

A5 ² Physikalisch-Technische Bundesanstalt (PTB), Abbestrasse 2-12, 10587 Berlin, Germany

A6 ³ Physikalisch-Technische Bundesanstalt (PTB), Bundesallee 100, 38116 Brunswick, Germany

A7 ⁴ Kirchhoff-Institute for Physics, Heidelberg University, Im Neuenheimer Feld 227,
A8 69120 Heidelberg, Germany

A9 ⁵ Present Address: Institut für Festkörperphysik - Abteilung Nanostrukturen, Gottfried Wilhelm
A10 Leibniz Universität Hannover, 30167 Hannover, Germany

21 **1 Introduction**

22 There are several fields, including radionuclide metrology, nuclear medicine and the
 23 nuclear power industry, that request improved knowledge of beta spectrum shapes.
 24 In principle, there are two ways to determine the shapes of beta spectra: theoret-
 25 ical calculation or experimental beta spectrometry. Calculations of spectra from
 26 forbidden, in particular, non-unique transitions are very complicated, and spectra
 27 published in the literature often reveal large discrepancies for one and the same
 28 radionuclide. The theoretical approaches for improved calculations must be verified
 29 against precise experimental data.

30 Metallic magnetic calorimeters (MMCs) with beta emitters enclosed in noble
 31 metal absorbers have demonstrated their potential for the study of beta spectrum
 32 shapes [1–3]. In the European Metrology Research Project MetroBeta [4], MMCs
 33 were optimized for the requirements in beta spectrometry, and three beta spectra
 34 covering different types of beta transition have been measured: ^{14}C (allowed), ^{151}Sm
 35 (first forbidden non-unique) and ^{99}Tc (second forbidden non-unique). Measurements
 36 of ^{36}Cl (second forbidden non-unique) are under way.

37 **2 Experimental**

38 **2.1 MMC beta Spectrometry System**

39 The development of MMCs within the project, optimized for absorber heat capac-
 40 ities ranging from 8 pJ/K to 1.7 nJ/K at 20 mK, has been described in Ref. [5].
 41 Figure 1 shows the design of the “M size” (110 pJ/K) MMC chip together with a

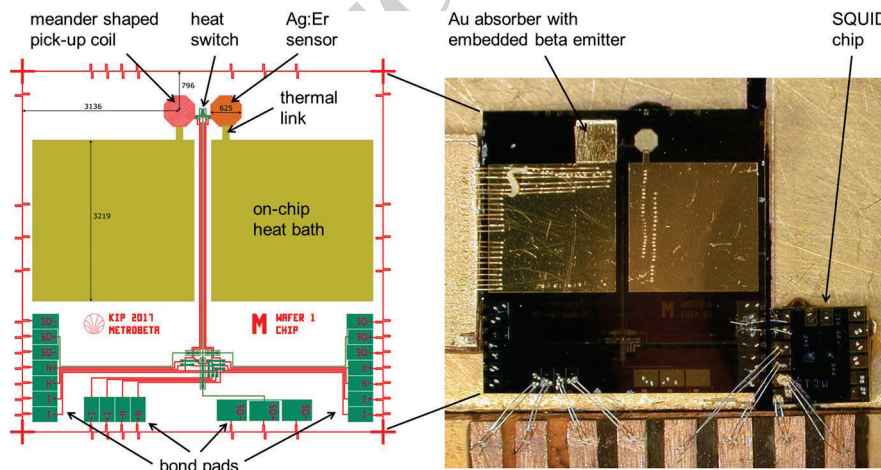


Fig. 1 *Left:* Design of the “M size” MMC chip. The chip size is $(7.2 \text{ mm})^2$. Some additional dimensions are given in the figure in μm ; the sensor measures $625 \mu\text{m}$ across. For further details, see Ref. [14]. *Right:* Photograph of a chip from the first fabricated batch; a gold absorber with an embedded beta emitter is placed on one of the Ag:Er sensors. (Color figure online)

42 photograph of a chip from the first fabricated batch. A gold absorber with an embed-
43 ded beta emitter is visible on one of the two Ag:Er sensors; it was fixed to the sensor
44 with Stycast 1266 epoxy resin. The SQUID reading out the MMC signal is placed
45 next to the MMC chip.

46 2.2 Source and Absorber Preparation Techniques

47 The source preparation is fundamental for the precise measurement of beta spectra
48 with MMCs. It must ensure that the entire energy of every beta particle is deposited
49 and thermalized in the absorber.

50 The best source preparation approach—besides implanting the radionuclide
51 directly into the absorber material—is electrodeposition forming a metallic layer.
52 For many elements, however, an oxide/hydroxide layer will form during electrodeposi-
53 tion. This can still be a high-quality source consisting in a very thin layer. Within
54 this project, ^{151}Sm and ^{99}Tc sources were fabricated by electrodeposition.

55 Where electrodeposition is not possible, as is the case of ^{14}C or ^{36}Cl , drop-deposi-
56 ted sources were produced. The common manual drop deposition often leads to the
57 formation of large (~micrometers) salt crystals. Previous studies using MMCs have
58 revealed that salt crystals can cause considerable spectrum distortion due to incom-
59 plete thermalization [6]. The formation of large salt crystals can be avoided if the
60 required activity is deposited in a 2D array of very small individual droplets. Com-
61 mercial micro-dispensing systems can deposit single droplet volumes of less than
62 50 pl in combination with a placement accuracy of better than 20 μm . With such a
63 system, ^{36}Cl , ^{99}Tc and ^{14}C were deposited onto gold foils preformed into absorber
64 arrays by milling techniques, with lateral dimensions of individual absorber ele-
65 ments of about 0.7 mm and 1.6 mm. Figure 2a shows an absorber array after the
66 radioactive solution was dried. Volumes of 100 nl (left half) and 50 nl (right half)
67 of a ^{99}Tc solution were deposited in the middle of each marked absorber. The

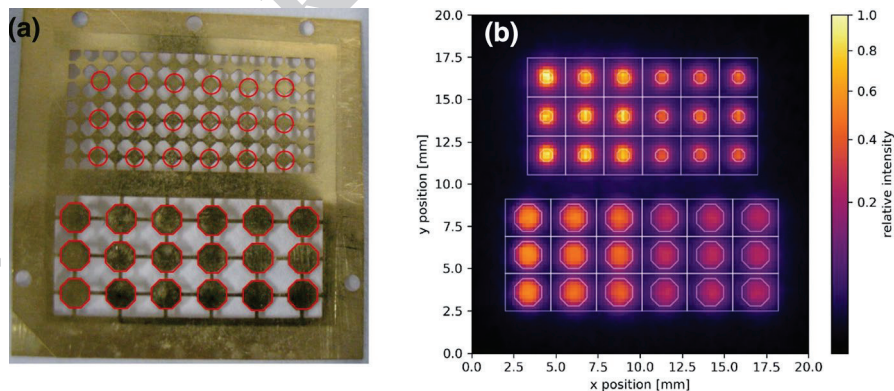


Fig. 2 **a** Photograph of an array of pre-fabricated gold absorber foils with ^{99}Tc sources deposited by a microdrop dispenser system in the middle of the marked absorbers. **b** Autoradiography image of the same array. Two different activity levels, 5 Bq/2.5 Bq, have been deposited on each marked absorber in the left/right half of the array. (Color figure online)

68 autoradiography image in Fig. 2b confirms the position and the different activities of
69 the deposited material.

70 Fine dispersion of the source material in the absorber metal will also improve
71 the source quality compared to a conventional drop-deposited source. This can be
72 achieved by alternate folding and laminating of the foil with the source deposit,
73 breaking the source crystals into tens of nanometer small particles that are embed-
74 ded in the metal foil [7]. This technique was applied to the electrodeposited ^{151}Sm
75 source, because it had a black aspect and was considered not to be ideally thin.

76 Monte Carlo simulations—see Sect. 4—indicate that spectrum distortion of
77 higher energy beta spectra by escape of bremsstrahlung from the absorber can be
78 reduced by embedding the beta emitter into bilayer absorbers with an inner layer of
79 lower atomic number and an outer layer of high atomic number (e.g., copper, $Z=29$,
80 and gold, $Z=79$). Preparing this kind of absorbers requires several steps of diffusion
81 welding under vacuum or inert gas to avoid oxidation of the copper.

82 3 Beta Spectrum Measurements

83 Three beta spectra have been measured using MMCs within the MetroBeta project;
84 the more challenging ^{36}Cl measurements are under way.

85 3.1 ^{14}C

86 The spectrum of ^{14}C ($Q=156.476$ keV) has been measured using a source prepared
87 as described in Ref. [5]. The absorber (Au, $1\text{ mm}^2 \times (2 \times 25\text{ }\mu\text{m})$) was placed on an **AQ3**
88 MMC chip best matching its heat capacity (34 pJ/K at 10 mK). The experimen-
89 tal conditions during the measurement were far from optimal. During the cooling
90 phase, the glue layer fixing the MMC chip to its holder broke; the chip was then
91 only suspended by the gold and aluminum bonding wires used for electric and ther-
92 mal contacts. Hence, the MMC could vibrate, resulting in an energy resolution near
93 200 eV (FWHM), approximately five times worse than expected from the absorber
94 heat capacity. Nevertheless, the detector performance was much better than in the
95 measurement published in [5]: The energy resolution was improved by a factor of
96 five, while the energy threshold was reduced from ~ 5 to ~ 700 eV. Figure 3 shows
97 the experimental spectrum containing 2.7 million events together with a theoretical
98 spectrum calculated with the code BetaShape [8, 9].

99 3.2 ^{151}Sm

100 A ^{151}Sm source was electrodeposited on a 10- μm -thick silver foil, forming a Sm
101 oxide/hydroxide layer. After the mechanical processing described in Sect. 2.2, this
102 source foil ($0.8\text{ mm} \times 0.8\text{ mm} \times 7\text{ }\mu\text{m}$) was sandwiched between two silver foils
103 ($0.9\text{ mm} \times 0.9\text{ mm} \times 15\text{ }\mu\text{m}$ each, total absorber heat capacity: 14.5 pJ/K at 10 mK).
104 The performance of the MMC during this measurement was as expected: The

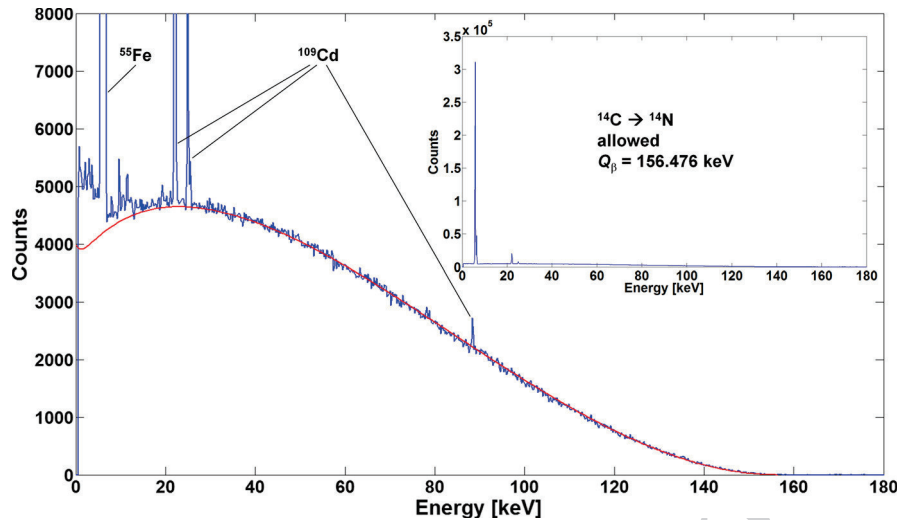


Fig. 3 Beta spectrum of ^{14}C measured with an MMC (blue). The discrete lines are X-ray and gamma ray lines from an external $^{55}\text{Fe} + ^{109}\text{Cd}$ energy calibration source. The inset shows the unclipped spectrum with the energy calibration lines in full height. A theoretical spectrum calculated with the code BetaShape is shown in red. The deviation of the experimental spectrum at low energies may be attributed to the degraded detector performance. (Color figure online)

105 energy resolution ranges from 45 eV (FWHM) at 6 keV to 70 eV at 25 keV, and the
 106 energy threshold is 250 eV.

107 ^{151}Sm has a main β^- decay branch ($Q_\beta = 76.4 \text{ keV}$) to the ground state and a sec-
 108 ond β^- decay branch to the 21.54 keV excited level of ^{151}Eu . The recommended val-
 109 ues for the probabilities of the two decay paths are 99.07 (4) % and 0.93 (4) % [10].
 110 The de-excitation of the 21.54 keV excited state leads to the emission of gamma rays
 111 (3.4% of the decays), respectively, to the emission of conversion electrons and sub-
 112 sequently X-rays and/or Auger electrons. The detector absorber stops all conversion
 113 electrons, more than 99% of all X-rays and more than 95% of the 21.54 keV gamma
 114 photons. The result is that for practically all beta decays to the excited level, the sum
 115 of the beta energy and the gamma energy is absorbed. Thus, the measured spectrum
 116 for the decays to the excited level is shifted by the energy of the gamma transition
 117 and starts at 21.54 keV, leading to a step in the recorded spectrum. Since the maxi-
 118 mum energy for this beta branch equals the Q value minus the gamma transition
 119 energy, the end point of both measured spectra is the same, 76.4 keV. As it is not
 120 possible to distinguish events from the two decay branches, both spectra are super-
 121 imposed in one experimental spectrum.

122 The measured spectrum (10.2 million events) is shown in Fig. 4 together with
 123 theoretical spectra calculated with the code BetaShape for both decay paths. The
 124 area between the two theoretical spectra, corresponding to the probability of the
 125 decay to the excited state of ^{151}Eu , amounts to 2.6% of the total, in clear contradic-
 126 tion with the recommended value. Concerning the spectrum shape, the discrepancy
 127 between experiment and theory at low energies is most likely due to an incomplete

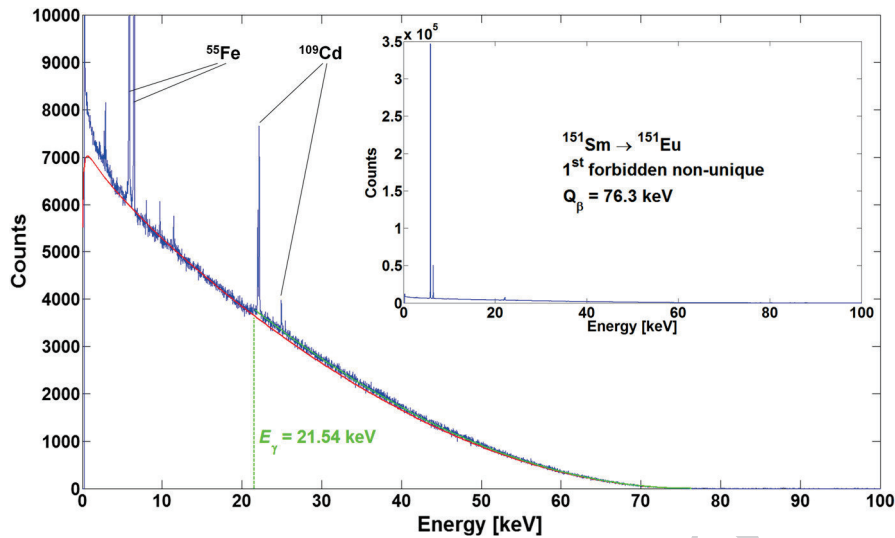


Fig. 4 Beta spectrum of ^{151}Sm measured with an MMC (blue) together with theoretical spectra calculated for the beta decay to the ground state (red) and to the 21.54 keV excited level of ^{151}Eu (green). The inset shows the unclipped spectrum with the energy calibration lines in full height. (Color figure online)

128 control of the atomic effects in the theoretical calculation of this first forbidden, non-
 129 unique transition.

130 3.3 ^{99}Tc

131 The beta spectrum of ^{99}Tc ($Q = 293.8 \text{ keV}$) was measured both at PTB and at LNHB.
 132 At LNHB, a ^{99}Tc source was electrodeposited on gold, forming metallic technetium.
 133 This source foil was sandwiched between two gold foils ($0.9 \text{ mm} \times 0.9$
 134 $\text{mm} \times 74 \mu\text{m}$ each, $C_{\text{abs}} = 175 \text{ pJ/K}$ at 10 mK). Data were acquired during 13.7 days,
 135 and the spectrum contains 5.65 million events. The energy resolution is practically
 136 energy independent, about 100 eV (FWHM) up to 384 keV , and the highest energy
 137 gamma line of a ^{133}Ba source used for energy calibration and check of the linearity.
 138 Comparing the measured and the tabulated line energies between 31 keV and
 139 384 keV shows no larger deviations than 70 eV , less than the energy resolution, and
 140 no obvious trend.

141 At PTB, ^{99}Tc sources were prepared with a microdrop dispenser directly on a
 142 $90\text{-}\mu\text{m}$ -thick gold absorber array (Fig. 2a). An identical array was diffusion welded
 143 onto the array with the sources. One of the larger absorbers ($C_{\text{abs}} = 545 \text{ pJ/K}$ at
 144 20 mK) was glued onto a matching MMC. The spectrum after 42 h of data acquisition
 145 consists of 0.5 million events with an energy threshold of about 5 keV and an
 146 energy resolution of 600 eV at the 122 keV gamma line of a ^{57}Co energy calibration
 147 source. The larger absorber heat capacity, vibrations from the pulse tube cooler and

148 bath temperature instability explain the degraded energy resolution and threshold
149 compared to the measurement performed at LNHB.

150 Figure 5 shows a superposition of both experimental spectra; the spectrum
151 shape is practically the same. The theoretical spectrum that is also shown in Fig. 5
152 has been calculated with the current version of the code BetaShape, supposing an
153 allowed transition, and multiplied with an experimental shape factor [11]. It is not
154 surprising that this shape factor, derived from a measurement with an energy thresh-
155 old of 55 keV, cannot correctly reproduce the spectrum at lower energies. It is note-
156 worthy that the spectrum measured at LNHB has an energy threshold of 650 eV.

157 4 Toward the Measurement of ^{36}Cl

158 For beta spectra with maximum energies higher than a few 100 keV, potential distortion
159 of the measured spectra by the escape of bremsstrahlung must be considered. In
160 first order, the radiative energy loss of the beta particles scales linearly with energy.
161 Hence, the higher the beta Q value, the stronger the spectrum distortion will be.
162 In principle, this distortion can be corrected for via Monte Carlo simulation; how-
163 ever, the bremsstrahlung cross sections needed for the simulations suffer from high
164 uncertainties.

165 Since the bremsstrahlung production scales with the square of the atomic num-
166 ber Z , a low Z absorber material may be a good candidate in view of minimizing
167 this source of spectrum distortion. On the other hand, a low Z absorber needs to

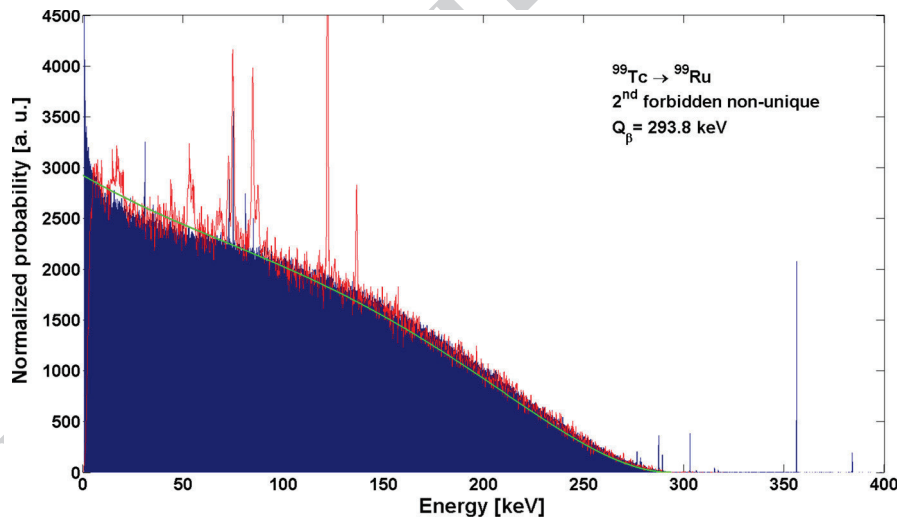


Fig. 5 Beta spectrum of ^{99}Tc resulting from two fully independent measurements and data analyses. *Blue histogram*: measured at LNHB (Laboratoire National Henri Becquerel, France) and *red line*: measured at PTB (Physikalisch-Technische Bundesanstalt, Germany). All lines in the blue spectrum are from a ^{133}Ba energy calibration source (including some escape peaks); all lines in the red spectrum are from a ^{57}Co energy calibration source. A theoretical spectrum calculated with the code BetaShape and using a shape factor from Ref. [11] is also shown (*green*). (Color figure online)

168 be significantly larger in order to stop the beta particles, thus implying larger heat
169 capacity, and is moreover less efficient for the reabsorption of at least a fraction
170 of the bremsstrahlung photons. A composite absorber composed of an inner layer
171 of a low Z material, reducing the bremsstrahlung production near the beta emitter
172 where the beta particles have still high energy, and an outer layer of a high Z material,
173 reducing the overall absorber heat capacity compared with a monolithic low
174 Z absorber and more efficiently reabsorbing photons, may be an interesting option
175 combining the advantages of both low and high Z .

176 To test this hypothesis, a series of Monte Carlo simulations have been performed
177 using the PENELOPE code [12] for the case of ^{36}Cl ($Q = 709.53$ keV). Five types of
178 absorber comprising elements with three different atomic numbers were simulated:
179 monolithic gold ($Z = 79$), silver ($Z = 47$) and copper ($Z = 29$), and composite absorbers
180 with an inner copper or silver layer and an outer gold layer. For each absorber
181 type, in a first step the minimal necessary absorber thickness was determined by
182 means of lower statistics simulations only at the maximum energy of ^{36}Cl . In a second
183 step, the resulting absorber was simulated with a central 100-nm-thick NaCl
184 layer acting as a source layer spiked with the active ^{36}Cl . Electrons with initial energies
185 following a theoretical spectrum based on the experimental ^{36}Cl spectrum from
186 Ref. [1] were generated in the source layer; the result of the simulation is the distribution
187 of the energies deposited in the absorber, i.e., the expected spectrum that
188 would be measured with each absorber.

189 Figure 6 presents the five simulated spectra together with the initial theoretical
190 spectrum. It can be clearly seen that the spectrum distortion is highest for the monolithic
191 gold absorber ($\sim 1.5\%$ in the energy range 100–200 keV) and becomes smaller
192 with lower Z . One can also observe that the spectrum distortion in the composite
193 silver (resp. copper)–gold absorber is smaller than in the monolithic silver (resp.
194 copper) absorber. The smallest distortion is obtained with the copper–gold bilayer
195 absorber.

196 A first attempt with a ^{36}Cl source prepared on a copper foil and embedded subsequently
197 between two copper–gold bilayers was made; unfortunately, the detector
198 did not perform as expected and no exploitable spectrum could be measured. New
199 measurements with both gold and copper–gold bilayer absorbers will be performed
200 shortly and compared with the Monte Carlo simulations.

201 5 Conclusions and Perspectives

202 Within the European Metrology Research Project MetroBeta, developments of both
203 MMCs and source/absorber preparation techniques for beta spectrometry have been
204 conducted. Several spectra with end-point energies ranging from ~ 76 to 294 keV
205 were measured, and the measurements of ^{36}Cl ($Q_{\beta} = 709$ keV) are ongoing. It was
206 demonstrated that MMC measurements also have the potential to yield valuable
207 information about other decay scheme parameters such as the probability of the beta
208 decay from ^{151}Sm to the excited level of ^{151}Eu . Thus, MMC spectrometry of radio-
209 nuclides with more complex decay schemes is an interesting extended research field

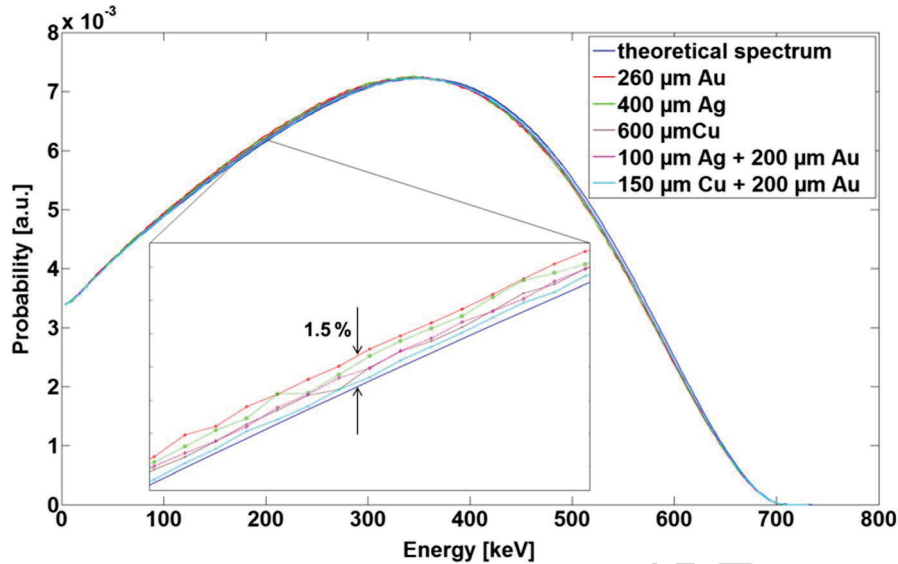


Fig. 6 Simulation of the spectrum distortion due to the escape of bremsstrahlung in the case of the beta spectrum of ^{36}Cl ($Q = 709.53$ keV). The initial spectrum based on Ref. [1] is shown in dark blue. Five types of absorbers were simulated: Au (red), Ag (green), Cu (brown), Ag–Au bilayer (magenta) and Cu–Au bilayer (cyan). The layer thicknesses are indicated in the figure. For better visibility, the inset shows a zoom into the energy range 150–200 keV. (Color figure online)

210 [13]. Studies indicate that ^{129}I , ^{204}Tl and ^{210}Pb are promising candidates for such
 211 measurements which should yield valuable nuclear decay data.

212 **Acknowledgements** This work was performed as part of the EMPIR Project 15SIB10 MetroBeta. The
 213 project has received funding from the EMPIR program co-financed by the Participating States and from
 214 the European Union's Horizon 2020 research and innovation program.

215 References

- 216 1. H. Rotzinger, M. Linck, A. Burck, M. Rodrigues, M. Loidl, E. Leblanc, L. Gastaldo, A. Fleis- AQ4
 217 chmann, C. Enss, J. Low Temp. Phys. **151**, 1087 (2008)
- 218 2. M. Loidl, M. Rodrigues, B. Censier, S. Kowalski, X. Mougeot, P. Cassette, T. Branger, D. Lacour,
 219 Appl. Radiat. Isot. **68**, 1454 (2010)
- 220 3. M. Loidl, C. Le-Bret, M. Rodrigues, X. Mougeot, J. Low Temp. Phys. **176**, 1040 (2014)
- 221 4. <http://metrobeta-empir.eu/>
- 222 5. M. Loidl, J. Beyer, L. Bockhorn, C. Enss, D. Györi, S. Kempf, K. Kossert, R. Mariam, O. Nähle, M.
 223 Paulsen, M. Rodrigues, M. Schmidt, J. Low Temp. Phys. **193**, 1251 (2018)
- 224 6. C. Le-Bret, M. Loidl, M. Rodrigues, X. Mougeot, J. Bouchard, J. Low Temp. Phys. **167**, 985 (2012)
- 225 7. A.S. Hoover et al., Anal. Chem. **87**, 3996–4000 (2015)
- 226 8. X. Mougeot, C. Bisch, Phys. Rev. A **90**, 012501 (2014)
- 227 9. X. Mougeot, Phys. Rev. C **92**, 059902 (2015)
- 228 10. M.-M. Bé et al., Table of Radionuclides, Monographie BIPM-5, vol. 8 (2016),
 229 ISBN-13 978-92-822-2264-5
- 230 11. M. Reich, H.M. Schüpferling, Z. Phys. **271**, 107–113 (1974)

- 231 12. F. Salvat et al., PENELOPE A code system for Monte Carlo simulation of Electron and Photon
232 transport, Rapport NEA/NSC/DOC (2001) 19
233 13. P. C.-O. Ranitzsch, D. Arnold, J. Beyer, L. Bockhorn, J. J. Bonaparte, C. Enss, K. Kossert, S.
234 Kempf, M. Loidl, R. Mariam, O. J. Nähle, M. Paulsen, M. Rodrigues, M. Wegner, J. Low Temp.
235 Phys. This Special Issue (2019)
236 14. S. Kempf, A. Fleischmann, L. Gastaldo, C. Enss, J. Low Temp. Phys. **193**, 365 (2018)

237 **Publisher's Note** Springer Nature remains neutral with regard to jurisdictional claims in published
238 maps and institutional affiliations.
239

Journal:	10909
Article:	2398

Author Query Form

Please ensure you fill out your response to the queries raised below and return this form along with your corrections

Dear Author

During the process of typesetting your article, the following queries have arisen. Please check your typeset proof carefully against the queries listed below and mark the necessary changes either directly on the proof/online grid or in the 'Author's response' area provided below

Query	Details Required	Author's Response
AQ1	Kindly check and confirm whether the mail ID is correctly identified.	
AQ2	Kindly check and confirm whether the corresponding author is correctly identified.	
AQ3	Kindly check and confirm the section headings are correctly identified.	
AQ4	As References 1 and 14 are same, we have deleted the duplicate reference and renumbered accordingly. Please check and confirm.	